Editors' Suggestion

Modular Analysis of Arbitrary Dipolar Scatterers

Viktar S. Asadchy[1,2,*] and Sergei A. Tretyakov[1]

[1] *Department of Electronics and Nanoengineering, Aalto University, P. O. Box 15500, FI-00076 Aalto, Finland*
[2] *Department of General Physics, Francisk Skorina Gomel State University, 246019 Gomel, Belarus*

(Received 2 November 2018; revised manuscript received 7 July 2019; published 28 August 2019)

Within the paradigm of metamaterials and metasurfaces, the electromagnetic properties of composite materials can be engineered by shaping or modulating their constituents, the so-called meta-atoms. Synthesis and analysis of complex-shaped meta-atoms with general polarization properties is a challenging task. In this paper, we demonstrate that the most general dipolar response of any small object can be conceptually decomposed into a set of basic fundamental polarization phenomena, which enables immediate all-direction characterization of the electromagnetic properties of arbitrary linear materials and metamaterials. The proposed platform for modular characterization is tested on several examples of bianisotropic and nonreciprocal meta-atoms. As a demonstration of the potential of this modular analysis, we use it to design a single-layer metasurface of vanishing thickness with unitary circular dichroism. The analysis approach developed in this paper is supported by a ready-to-use computational code and can be further extended to meta-atoms engineered for other types of wave interactions, such as in acoustics and mechanics.

DOI: 10.1103/PhysRevApplied.12.024059

I. INTRODUCTION

Metamaterials are engineered composites consisting of tailored subwavelength meta-atoms (inclusions) for controlling wave phenomena at will. During the last two decades, metamaterials have attracted great interest from researchers working in different fields of physics, which has resulted in an important impact on fundamental science and the emergence of numerous fascinating concepts [1–5]. Nevertheless, there is no universal approach to the synthesis of arbitrary complex metamaterials, mainly due to the two following reasons. First, determining the required properties of single meta-atoms in a composite is a complicated inverse problem due to their mutual interactions. Second, even if such properties are known, the practical realization of meta-atoms can still be very challenging because it implies rigorous design and optimization of their anisotropic properties, i.e., their entire polarizability tensors. For this reason, the vast majority of work in the literature has been devoted to metamaterials whose functionality is engineered for only a small number (usually only one) of specific illumination directions. For example, multipole analysis methods [6–9] provide information on only the cross sections of meta-atoms for particular excitations. Meanwhile, the properties of metamaterials excited by fields of other configurations remain unknown and unprescribed. However, such knowledge is often very important and can lead to unexpected and unique phenomena, as was demonstrated by the example of planar chirality [10–14], which occurs only at specific oblique-angle illuminations, in contrast to true three-dimensional chirality. Furthermore, in many situations, one needs to know under what excitation a meta-atom will respond in some particular way, for example, exhibiting the highest possible Willis coupling [15], the strongest mechanical twist [16], a desired asymmetry [12,17], or pronounced nonreciprocal properties [18]. Such *arbitrary-illumination* analysis, once developed, would be very beneficial for the understanding and even design of bulk metamaterials and their two-dimensional counterparts (metasurfaces [19,20]) intended to interact with waves of arbitrary nature: acoustic, electromagnetic, mechanical, etc.

In this paper, a universal platform for analyzing the properties of arbitrarily complex linear meta-atoms and other small objects is proposed. Although we present results for meta-atoms designed for interactions with electromagnetic waves, the same approach can be used for the analysis of other types of wave interactions. We show that the response of a general linear meta-atom can be thought of as a combination of the responses of several basic modules with known fundamental electromagnetic properties, immediately revealing the properties of the meta-atom for all possible excitations. Figure 1 depicts a conceptual illustration of such a decomposition. This platform for a

*asadchy@stanford.edu

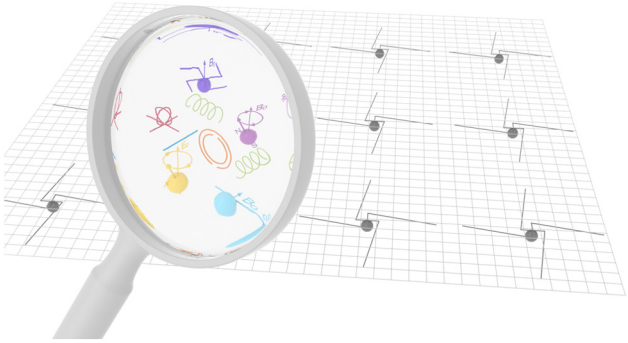

FIG. 1. Conceptual illustration of the proposed modular analysis. An arbitrary scatterer (located in a two-dimensional array of equivalent scatterers in this case) with a complex polarization response is decomposed into a combination of responses from several basic modules with known electromagnetic properties.

transition from complex material units to basic elements is in a sense analogous to what is done in electronics, where an arbitrarily complex linear circuit is represented as a network of basic elements: capacitors, inductors, resistors, and gyrators. There is also some analogy with the recently introduced "metatronics" [21], which relies on the decomposition of complex electromagnetic systems into elementary scatterers with simple dispersion properties. In electronics, when a complex circuit is represented as a combination of lumped elements, it becomes apparent what kinds of elements of what strength must be added or removed to improve or optimize the desired response. Likewise, our proposed modular analysis can also serve as a powerful tool for the *synthesis* and *optimization* of meta-atoms with required polarization properties. Importantly, the proposed concept is not limited to physically engineered materials (metamaterials). It is applicable to any objects that are small enough (responding as a set of dipoles), such as the usual molecules, atoms, and other electrically or optically small objects. The only assumptions exploited in the concept are linearity and the dipolar response.

In what follows, we successfully test the proposed modular analysis on several examples of dipolar meta-atoms with general electromagnetic properties, including bianisotropy and nonreciprocity. It is demonstrated further, using an example of a split-ring resonator, how the platform can be used for designing (synthesizing) meta-atoms and metasurfaces with maximized (or minimized) desired effects. For the convenience of the reader, the analysis approach developed in this paper is supported by a ready-to-use code and program files (including a tutorial video showing a step-by-step procedure for a split-ring resonator) [22,23]. The code and program files provide automation for obtaining results for a meta-atom with an arbitrary customer-defined geometry.

II. MODULAR DECOMPOSITION OF POLARIZATION EFFECTS

Let us first consider an arbitrary single meta-atom located in free space so that its interaction with other meta-atoms can be neglected. Its electromagnetic response is assumed to be linear and dipolar, which is the case for most inclusions in engineered metamaterials and metasurfaces. No assumptions about its reciprocity or anisotropy properties are made, meaning that in the general case it can be bianisotropic and nonreciprocal. Thus, the electromagnetic properties of the meta-atom are characterized by four polarizability dyadics (tensors), namely an electric one, $\overline{\overline{\alpha}}_{\rm ee}$, an electromagnetic one, $\overline{\overline{\alpha}}_{\rm em}$, a magnetoelectric one, $\overline{\overline{\alpha}}_{\rm me}$, and a magnetic one, $\overline{\overline{\alpha}}_{\rm mm}$, including in total 36 complex polarizability components. To apply modular analysis to the meta-atom, one needs first to determine all these components. Several techniques for polarizability extraction have been proposed during the last decade [24–28], but none of them allows calculation of all the polarizability components simultaneously. In this paper, the approach based on scattered-far-field probing [25] is extended [22] and utilized. It should be noted that even in cases when the unknown meta-atom cannot be described solely by dipolar moments, the modular analysis can still be done using an alternative T-matrix formulation which takes into account higher-order multipoles [6–8].

When the four polarizability dyadics of the meta-atom are determined, it is important to differentiate between reciprocal and possible nonreciprocal polarization properties. Using the Onsager-Casimir symmetry relations for bianisotropic meta-atoms [29] $\overline{\overline{\alpha}}_{\rm ee}(H_0)=\overline{\overline{\alpha}}^{\,T}_{\rm ee}(-H_0)$, $\overline{\overline{\alpha}}_{\rm mm}(H_0)=\overline{\overline{\alpha}}^{\,T}_{\rm mm}(-H_0)$, and $\overline{\overline{\alpha}}_{\rm em}(H_0)=-\overline{\overline{\alpha}}^{\,T}_{\rm me}(-H_0)$, one can represent each of the dyadics $\overline{\overline{\alpha}}_{\rm ee}$, $\overline{\overline{\alpha}}_{\rm em}$, $\overline{\overline{\alpha}}_{\rm me}$, and $\overline{\overline{\alpha}}_{\rm mm}$ as a sum of reciprocal and nonreciprocal parts (here, T is the transpose operation, H_0 denotes all external nonreciprocal parameters such as a bias magnetic field or an angular velocity, and $-H_0$ corresponds to the case when the signs of all these parameters are reversed). These reciprocal (subscript r) and nonreciprocal (subscript n) parts read

$$\overline{\overline{\alpha}}_{{\rm ee},r}=\frac{\overline{\overline{\alpha}}_{\rm ee}+\overline{\overline{\alpha}}^{\,T}_{\rm ee}}{2},\qquad \overline{\overline{\alpha}}_{{\rm ee},n}=\frac{\overline{\overline{\alpha}}_{\rm ee}-\overline{\overline{\alpha}}^{\,T}_{\rm ee}}{2},$$
$$\overline{\overline{\alpha}}_{{\rm mm},r}=\frac{\overline{\overline{\alpha}}_{\rm mm}+\overline{\overline{\alpha}}^{\,T}_{\rm mm}}{2},\qquad \overline{\overline{\alpha}}_{{\rm mm},n}=\frac{\overline{\overline{\alpha}}_{\rm mm}-\overline{\overline{\alpha}}^{\,T}_{\rm mm}}{2}, \tag{1}$$

$$\overline{\overline{\alpha}}_{{\rm em},r}=\frac{\overline{\overline{\alpha}}_{\rm em}-\overline{\overline{\alpha}}^{\,T}_{\rm me}}{2},\qquad \overline{\overline{\alpha}}_{{\rm em},n}=\frac{\overline{\overline{\alpha}}_{\rm em}+\overline{\overline{\alpha}}^{\,T}_{\rm me}}{2}. \tag{2}$$

The magnetoelectric dyadic $\overline{\overline{\alpha}}_{\rm me}$ is excluded from Eq. (1) since it is fully determined by $\overline{\overline{\alpha}}_{\rm em}$. It should be noticed that the dyadics $\overline{\overline{\alpha}}_{{\rm ee},r}$ and $\overline{\overline{\alpha}}_{{\rm mm},r}$ are symmetric, while $\overline{\overline{\alpha}}_{{\rm ee},n}$ and $\overline{\overline{\alpha}}_{{\rm mm},n}$ are antisymmetric. However, both the reciprocal and

the nonreciprocal electromagnetic dyadics have symmetric and antisymmetric parts.

Any symmetric dyadic (e.g., $\bar{\bar{\alpha}}_{ee,r}$) can always be represented as a linear combination of a diagonal dyadic in the initial *xyz* basis and another diagonal dyadic in another basis given by the complex basis vectors $\mathbf{u}_1$, $\mathbf{u}_2$, and $\mathbf{u}_3$ [30]:

$$\bar{\bar{\alpha}}_{ee,r} = \bar{\bar{I}}(\alpha_{ee}^{xx} + \alpha_{ee}^{yy} + \alpha_{ee}^{zz})/3 + \sum_i \lambda_i \mathbf{u}_i \mathbf{u}_i, \qquad (3)$$

where $\bar{\bar{I}} = \mathbf{x}\,\mathbf{x} + \mathbf{y}\,\mathbf{y} + \mathbf{z}\,\mathbf{z}$ is the unit dyadic, $i = 1, 2, 3$; λ_i are complex coefficients such that $\sum_i \lambda_i = 0$; and the notation $\mathbf{u}_i\mathbf{u}_i$ denotes the dyadic product of two vectors (the same as a dyad). The first diagonal dyadic in Eq. (3) describes an isotropic electric response. The second dyadic is diagonal with zero trace in the basis of complex unit vectors. For a clear geometrical description, it is convenient to rewrite it as a linear combination of six dyadic products of real vectors in the initial basis with complex magnitudes S_j ($j = 1, 2, \ldots, 6$):

$$\sum_i \lambda_i \mathbf{u}_i \mathbf{u}_i = S_1 \mathbf{x}\,\mathbf{x} + S_2 \mathbf{y}\,\mathbf{y} + S_3 \mathbf{z}\,\mathbf{z} + \frac{S_4}{2}(\mathbf{x}+\mathbf{y})(\mathbf{x}+\mathbf{y}) + \frac{S_5}{2}(\mathbf{x}+\mathbf{z})(\mathbf{x}+\mathbf{z}) + \frac{S_6}{2}(\mathbf{y}+\mathbf{z})(\mathbf{y}+\mathbf{z}). \qquad (4)$$

The complex amplitude coefficients S_j can be determined based on the extracted polarizability dyadics (see the derivation in Ref. [22]).

Combining Eqs. (3) and (4), any symmetric dyadic in the general case is decomposed into six symmetric dyads (dyadic products of real vectors), all with different complex amplitudes. Thus, the response described by any reciprocal electric dyadic $\bar{\bar{\alpha}}_{ee,r}$ is equivalent to the response of a set of six basic modules which possess only one simple polarization response: they develop an electric dipole moment along a given direction when excited by an electric field along the same direction. For visualization purposes, we show these modules as straight needles, as shown in Fig. 2(a), spatially separating them for clarity. Three needles are oriented along the initial basis vectors and the other three along the bisectors of the angles between these axes. It should be noted that such a decomposition is not unique, and in most cases, as will be seen below, several of the modules may have negligible weights, which reduces their total number. All the needles have different complex polarization amplitudes. Hereafter, the amplitudes of the polarizability components are shown graphically as proportional to the *linear* dimension of the module and not to its volume. Now, the polarization properties of a meta-atom with $\bar{\bar{\alpha}}_{ee,r}$ given by Eq. (3) can be readily determined from Fig. 2(a). We see that, for example, an incident *x*-polarized plane wave will induce polarization currents and dipole moments simultaneously in three modules, resulting in polarization of the meta-atom along the

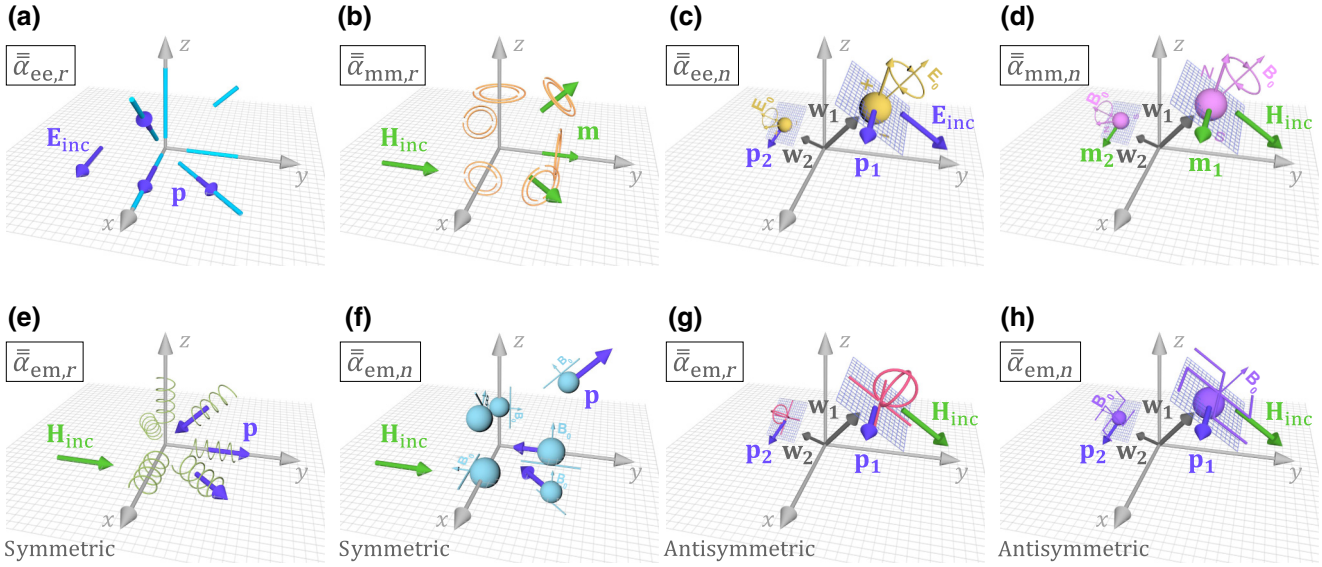

FIG. 2. Conceptual illustration of modular decomposition of different polarizability dyadics for an arbitrary dipolar meta-atom. The incident electric and magnetic fields are denoted by $\mathbf{E}_{inc}$ and $\mathbf{H}_{inc}$, while $\mathbf{p}$ and $\mathbf{m}$ are the induced electric and magnetic dipole moments. The additional planes drawn in the antisymmetric modules are orthogonal to their symmetry axes. Panels (a) and (b) depict the decomposition of general reciprocal electric and magnetic dyadics, respectively. The corresponding nonreciprocal dyadics are modeled by the basic meta-atoms shown in (c) and (d). The reciprocal bianisotropic dyadic in the general case is represented by the basic blocks shown in (e) and (g), while its nonreciprocal counterpart is described by the meta-atoms in (f) and (h).

x, y, and z axes (the phases of the polarization currents can be arbitrary). In this way, we can completely describe the electromagnetic properties of any meta-atom by only the types of the modules, their orientations, and the response strength of the individual modules.

Similarly, the symmetric dyadic $\overline{\overline{\alpha}}_{\mathrm{mm},r}$ is decomposed into six dyads according to Eqs. (3) and (4) (naturally, in general, with different complex amplitudes). Each decomposition term physically corresponds to a module which is reciprocal and polarizable only magnetically, only along one direction, and only by magnetic fields. For visualization purposes, we show the orientations and amplitudes of these modules by double split-ring resonators [31,32], because this type of polarization response is dominant for that shape (obviously, the response of such resonators is more complicated, and the modular decomposition of an actual double split-ring resonator can be found in Ref. [22]). Thus, the dyadic $\overline{\overline{\alpha}}_{\mathrm{mm},r}$ can be modeled as a combination of six different idealized double split-ring resonators, as illustrated in Fig. 2(b).

Any antisymmetric dyadic, such as $\overline{\overline{\alpha}}_{\mathrm{ee},n}$, can always be represented as a cross product of a complex vector and the unit dyadic (the complex vector is decomposed into two real vectors, with real amplitude A_1 and with imaginary amplitude jA_2) [30]:

$$\overline{\overline{\alpha}}_{\mathrm{ee},n} = \frac{1}{2}[(\alpha_{\mathrm{ee}}^{xy} - \alpha_{\mathrm{ee}}^{yx})(\mathbf{x}\,\mathbf{y} - \mathbf{y}\,\mathbf{x}) + (\alpha_{\mathrm{ee}}^{xz} - \alpha_{\mathrm{ee}}^{zx})(\mathbf{x}\,\mathbf{z} - \mathbf{z}\,\mathbf{x}) + (\alpha_{\mathrm{ee}}^{yz} - \alpha_{\mathrm{ee}}^{zy})(\mathbf{y}\,\mathbf{z} - \mathbf{z}\,\mathbf{y})] = A_1\mathbf{w}_1 \times \overline{\overline{I}} + jA_2\mathbf{w}_2 \times \overline{\overline{I}}. \tag{5}$$

The unknown coefficients A_1 and A_2 and vectors $\mathbf{w}_1$ and $\mathbf{w}_2$ are calculated in Ref. [22]. The two dyadics in Eq. (5) describe two uniaxial (with one symmetry axis) modules in which polarization occurs in the direction orthogonal to the incident field and to the symmetry axis of the module. The physical interpretation of each such module in the case of the nonreciprocal dyadic $\overline{\overline{\alpha}}_{\mathrm{ee},n}$ is an electric dipole precessing in a static external electric field $\mathbf{E}_0$ [see Fig. 2(c)]. The induced electric dipole is always perpendicular to the electric field of the incident wave. The nonreciprocal magnetic dyadic $\overline{\overline{\alpha}}_{\mathrm{mm},n}$, likewise, is modeled by two magnetic dipoles precessing in a static magnetic field $\mathbf{B}_0$ [see Fig. 2(d)].

Next, one needs to decompose the electromagnetic dyadics $\overline{\overline{\alpha}}_{\mathrm{em},r}$ and $\overline{\overline{\alpha}}_{\mathrm{em},n}$, which have symmetric and antisymmetric parts and describe the bianisotropic response of the meta-atom. The symmetric part of the former dyadic is equal to $(\overline{\overline{\alpha}}_{\mathrm{em}} + \overline{\overline{\alpha}}_{\mathrm{em}}^{T} - \overline{\overline{\alpha}}_{\mathrm{me}} - \overline{\overline{\alpha}}_{\mathrm{me}}^{T})/4$ and, according to Eqs. (3) and (4), is modeled by six modules with a uniaxial chiral bianisotropic response: for visual representation, thin multiturn metal helices [see Fig. 2(e)] are appropriate shapes to denote this fundamental polarizability effect. In general, we need two such chiral modules: right-handed and left-handed. An incident magnetic field tangential to the helix axis generates an electric polarization according to Faraday's law [33]. Likewise, the symmetric part of the dyadic $\overline{\overline{\alpha}}_{\mathrm{em},n}$, equal to $(\overline{\overline{\alpha}}_{\mathrm{em}} + \overline{\overline{\alpha}}_{\mathrm{em}}^{T} + \overline{\overline{\alpha}}_{\mathrm{me}} + \overline{\overline{\alpha}}_{\mathrm{me}}^{T})/4$, is represented by six uniaxial nonreciprocal modules [see Fig. 2(f)]. The effect of bianisotropic nonreciprocal coupling is strong in a meta-atom formed from a ferrite sphere covered by a metal wire (a so-called Tellegen meta-atom) [34–36], and we use an image of this meta-atom as a notation for the presence of this fundamental block in the decomposition. An incident alternating magnetic field creates a cross-polarized magnetization in the sphere (due to the off-diagonal permeability components of ferrite), which in turn results in an induced electric polarization of the wire (parallel to the alternating magnetic field).

The antisymmetric part of $\overline{\overline{\alpha}}_{\mathrm{em},r}$, expressed as $(\overline{\overline{\alpha}}_{\mathrm{em}} - \overline{\overline{\alpha}}_{\mathrm{em}}^{T} + \overline{\overline{\alpha}}_{\mathrm{me}} - \overline{\overline{\alpha}}_{\mathrm{me}}^{T})/4$, is modeled according to Eq. (5) by two uniaxial bianisotropic asymmetric modules (one with a real polarizability and another with an imaginary polarizability), which we show as crossed omega-shaped wires [37]; see Fig. 2(g). An incident magnetic field orthogonal to the module axis excites a mutually orthogonal electric polarization (due to Faraday's law and the specific wire shape). The last part in the modular decomposition is the antisymmetric part of $\overline{\overline{\alpha}}_{\mathrm{em},n}$, which can be calculated as $(\overline{\overline{\alpha}}_{\mathrm{em}} - \overline{\overline{\alpha}}_{\mathrm{em}}^{T} - \overline{\overline{\alpha}}_{\mathrm{me}} + \overline{\overline{\alpha}}_{\mathrm{me}}^{T})/4$. Two nonreciprocal modules based on a ferrite sphere with swastika-shaped metal wires [38] [shown in Fig. 2(h)] can represent the required polarization properties.

III. MODULAR DECOMPOSITION OF A SPLIT-RING RESONATOR

Next, as all the polarizability dyadics $\overline{\overline{\alpha}}_{\mathrm{ee}}$, $\overline{\overline{\alpha}}_{\mathrm{em}}$, $\overline{\overline{\alpha}}_{\mathrm{me}}$, and $\overline{\overline{\alpha}}_{\mathrm{mm}}$ have been decomposed into basic modules, the universality of the modular-decomposition concept can be demonstrated via the analysis of several realistic meta-atoms. The analysis for each of them is performed in three automated steps: extraction of the full polarizability dyadics of the unknown meta-atom [22] (performed using a full-wave simulator [39]), decomposition of the extracted polarizability dyadics (using computational software [40]), and three-dimensional visualization of the modules obtained (using the full-wave simulator). All the supporting files for a ready-to-use automated analysis of an unknown meta-atom can be found in Ref. [22] (together with a tutorial video showing the step-by-step procedure).

First, the modular analysis is applied to a split-ring resonator (SRR), as an example. The geometry and orientation of the SRR (shown in gray) in the initial basis can be seen in Fig. 3(a). The radius of the ring is 2.7 mm, the radius of the copper wire is 0.2 mm, and the gap is 0.4 mm. The decomposition is performed at the main resonance frequency of the SRR, 7.9 GHz. The power of

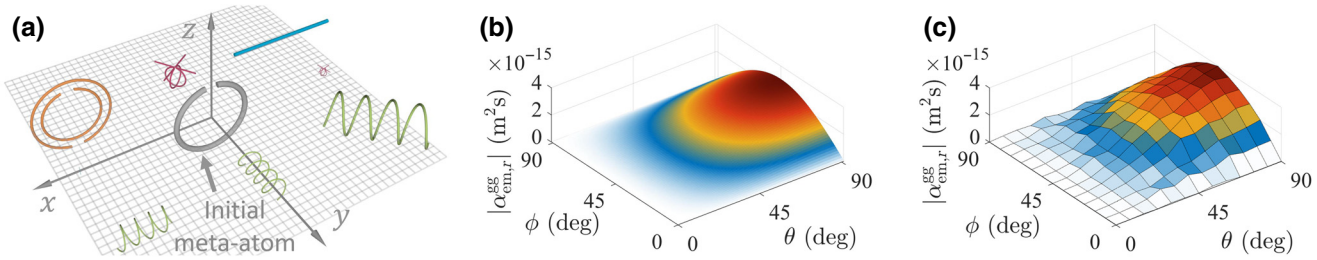

FIG. 3. (a) Modular decomposition of a split-ring resonator at its fundamental resonance. The linear dimensions of the modules are proportional to the amplitudes of the corresponding polarization effects. Surface plot illustrating the angular dependence of the amplitude of the chiral polarizability component $\alpha^{\mathrm{gg}}_{\mathrm{em},r} = \mathbf{g} \cdot \overline{\overline{\alpha}}_{\mathrm{em},r} \cdot \mathbf{g}$ of an SRR meta-atom with respect to the direction parallel to the unit vector $\mathbf{g}$. Results obtained from the modular decomposition (b), and results obtained using numerical full-wave simulations (c). The maximum chirality is observed when the external electric field is oriented at $\theta = 90^\circ$ and $\phi = 45^\circ$; the SRR effectively behaves as a left-handed helix oriented at these angles.

the modular analysis is evident from Fig. 3(a), where the electromagnetic response of the meta-atom can be immediately inspected for arbitrary illuminations. The strong electric polarization response along the x axis (straight wire) and the magnetic polarization along the y axis (magnetic module shown as a double SRR) are expected. However, additionally, the SRR exhibits a perceptible omega bianisotropic response when illuminated along the z axis [12,17] with a specific polarization of the incident wave [41]. In fact, the decomposition includes two uniaxial omega modules, one representing the purely real part of the polarizability and the other the purely imaginary part. Moreover, the decomposition includes two left-handed helices and one right-handed one, indicating strong chiral properties of the SRR. Although the total chirality is zero (the left- and right-handed helices precisely compensate each other, leading to vanishing three-dimensional chirality), for specific illumination directions one can excite predominantly left- or right-handed helices, achieving a nonzero chiral effect with a planar structure (the SRR can be *infinitesimally* thin, supporting only electric current). Planar chirality was observed earlier in various asymmetric structures [10–14]; however, this effect remained rather weak [14,42]. Using the modular decomposition, one can determine the chirality strength exhibited by the SRR for various orientations of the incident electric field. As is theoretically shown in Ref. [22], the maximum chirality is achieved when the electric field is along the unit vector $\mathbf{g} = \sin\theta\cos\phi\mathbf{x} + \sin\theta\sin\phi\mathbf{y} + \cos\theta\mathbf{z}$, where $\theta = 90^\circ$ and $\phi = \pm 45^\circ$ (the double sign is due to the mirror symmetry of the SRR with respect to the yz plane). Figure 3(b) depicts the theoretically calculated axial chiral polarizability of the split-ring resonator for different orientations of the incident electric field. The maximum of the chirality is observed at $\theta = 90^\circ$ and $\phi = 45^\circ$. To verify this theoretical result, the polarizability $\overline{\overline{\alpha}}_{\mathrm{em},r}$ is calculated using the abovementioned extraction technique, separately for each orientation of the incident electric field in the range of $\theta = [0^\circ, 90^\circ]$ and $\phi = [0^\circ, 90^\circ]$ with a step size of 7.5°. The results are depicted in Fig. 3(c) and are in close agreement with the theoretical ones in Fig. 3(b). The deviation in the peak amplitude value between these two figures (around 30%) can be explained by errors (which are of the order of 26% for this meta-atom) in the polarizability extraction.

As can be seen from Fig. 3(a), the SRR behaves differently for opposite illumination directions: as a left-handed helix when illuminated along the $(\mathbf{x} - \mathbf{y})$ direction (the right-handed helix in the decomposition in Fig. 3(a) is not excited) and as a right-handed helix when illuminated along the $(-\mathbf{x} - \mathbf{y})$ direction.

By performing modular decomposition for a meta-atom at different frequencies, one can analyze in more detail the evolution of its modules, specifically, their orientations and their weights in the decomposition. Next, we apply the decomposition for the split-ring resonator for a frequency sweep from 7 to 8.8 GHz. The results can be found as a video file in the Supplemental Material [22]. From the video, it can be clearly seen that the electric module along the x axis [the metallic needle in Fig. 3(a)] has nearly the same *weight* over the entire range (naturally, its absolute strength changes since the SRR is a resonant structure). On the other hand, the magnetic module and three chiral modules gain in weight as the frequency increases or, alternatively, decrease in weight at low frequencies. This result is in agreement with the fact that in the low-frequency limit the electric polarizability tends to a constant value while the magnetoelectric (as an effect of spatial dispersion) and magnetic polarizabilities are proportional to ω and ω^2, respectively [[43], p. 131]. From the video, one can observe that when the frequency sweeps from low to high through the resonance, the purely imaginary omega module [shown in Fig. 3(a) on the right-hand side] first grows in the region of normal frequency dispersion, then scales down in the region of anomalous frequency dispersion, and finally grows again. The purely real omega module, responsible for the scattering loss, is maximum at the resonance. This evolution clearly resembles the Lorentzian

frequency dispersion of the magnetoelectric polarizability. Finally, one can see in the video that, although not present in the decomposition at the resonance in Fig. 3(a), an additional electric module oriented along the z axis appears at low and high frequencies. Interestingly, exactly at the resonance, this module vanishes due to the symmetry of the current distribution in the wire of the SRR.

IV. DESIGN OF NEGLIGIBLY THIN METASURFACE WITH EXTREME CIRCULAR DICHROISM

The applicability of the modular analysis can be further demonstrated by designing a periodic metasurface made up of SRRs with the dimensions listed in the previous section. The metasurface has a subwavelength square unit cell with a 10-mm side. The SRRs are *parallel* to the metasurface plane. In contrast to conventional chiral metasurfaces relying on a finite thickness and a three-dimensional topology with broken space-inversion symmetry, the designed metasurface exhibits strong circular dichroism (and other chiral effects) with a pure two-dimensional geometry and negligible thickness. The metasurface is illuminated by circularly polarized plane waves at an angle $\phi = 45^\circ$ from the normal [$\mathbf{k}_{\rm inc} \uparrow\uparrow (\mathbf{x} - \mathbf{y})$ in the initial basis], as shown in the inset of Fig. 4. For this illumination, the right-handed helix shown in Fig. 3(a) is not excited, while both left-handed helical modules are activated. Thus, the SRR behaves for this illumination as a left-handed chiral meta-atom. The plot in the figure shows the frequency dispersion of the transmittance for right ("++") and left ("−−") circular polarizations of incident waves from full-wave simulations. At the resonance frequency of 8.23 GHz, the metasurface nearly fully transmits an incident right circular polarization and completely reflects waves of the opposite handedness (transforming their polarization). The cross-polarization transmittance ($|T_{+-}|^2$ and $|T_{-+}|^2$) of

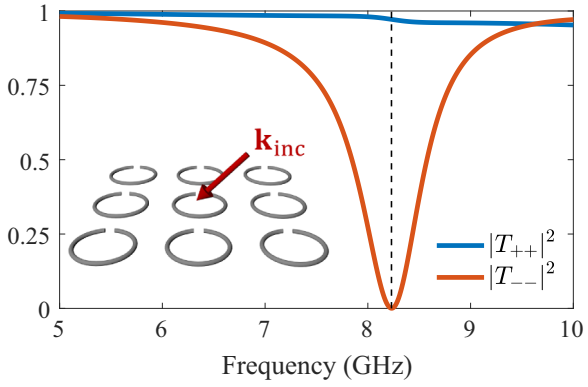

FIG. 4. Transmittance through a metasurface composed of SRRs for right ("++") and left ("−−") circularly polarized incident waves. The inset depicts the geometry of the metasurface and the wave vector $\mathbf{k}_{\rm inc}$ of incidence.

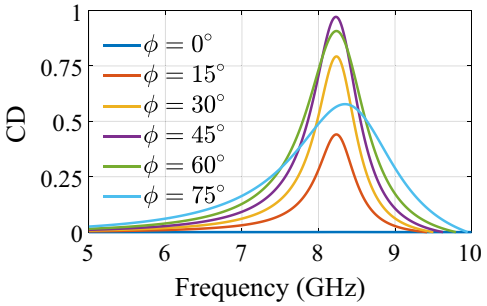

FIG. 5. Circular dichroism, defined as $\mathrm{CD} = |T_{++}|^2 + |T_{-+}|^2 - |T_{--}|^2 - |T_{+-}|^2$, of the metasurface versus frequency for different illumination angles ϕ.

the metasurface is indistinguishable from zero within the entire frequency range studied. As a figure of merit for different extinctions of right and left circular polarizations, we define the circular dichroism here as $\mathrm{CD} = |T_{++}|^2 + |T_{-+}|^2 - |T_{--}|^2 - |T_{+-}|^2$. This definition of the circular dichroism differs from the conventional one, written in terms of absorption coefficients. Our definition serves as a generalized chirality measure, applicable to both lossy and lossless structures. Figure 5 shows CD for the designed metasurface at different illumination angles. The maximum value of CD is achieved for $\phi = 45^\circ$, reaching a value of nearly unity. This is an exceptional result taking into account the negligible thickness of the metasurface. Such a high CD significantly exceeds the values reported in the literature for planar structures to date [14,42]. For normal incidence ($\phi = 0^\circ$), as expected, CD is zero.

The effect of planar chirality achieved with the designed metasurface should be distinguished from the anisotropy effect observed in planar dielectric metasurfaces [44]. In the latter case, a metasurface exhibits a symmetric response in terms of the copolarized transmission $|T_{++}| = |T_{--}|$ and an asymmetry for the cross-polarized transmission $|T_{+-}| \neq |T_{-+}|$.

V. MODULAR DECOMPOSITION OF A NONRECIPROCAL VIRTUALLY MOVING META-ATOM

In this section, modular decomposition is applied to a nonreciprocal meta-atom which can be used as a constituent of metasurface-based isolators and phase shifters. The geometry of the meta-atom is adopted from Ref. [18] and is shown in Fig. 6(a). The length of the copper wire is 30 mm, and the wire radius is 0.05 mm. The ferrite sphere, of radius 1.65 mm, is made of yttrium iron garnet with a relative permittivity of 15, the dielectric loss tangent is 10^{-4}, the saturation magnetization is 1780 G, and the full resonance linewidth is 0.2 Oe. The meta-atom is biased by an external $+z$-oriented permanent magnetic field of 9626 A/m. The magnetic resonance frequency at

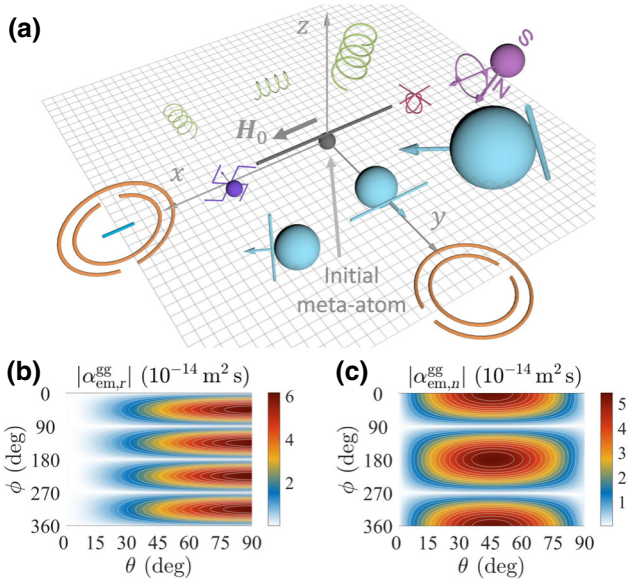

FIG. 6. (a) Modular decomposition of a nonreciprocal meta-atom (shown in gray) at its magnetic resonance frequency. Surface plots depicting (b) axial chiral and (c) Tellegen polarizabilities for different orientations of the incident electric field in a spherical coordinate system. The maximum chirality is observed when the electric field is oriented at $\theta = 90^\circ$ and $\phi = (45^\circ + 90^\circ N)$, and the maximum Tellegen properties at $\theta = 45^\circ$ and $\phi = 180^\circ N$.

which the modular analysis is performed is 1.975 GHz. The orientation of the magnetic bias field is along the $+x$ direction.

As was theoretically demonstrated in Refs. [[45], Eqs. (11)–(12)] and [46], *passive* metasurfaces that operate as highly efficient nonreciprocal phase shifters or isolators at normal incidence must consist of meta-atoms which possess predominantly artificial "moving" bianisotropic coupling (i.e., the entire dyadic $\overline{\overline{\alpha}}_{em}$ must be represented solely by the nonreciprocal antisymmetric part $\overline{\overline{\alpha}}_{em,n}$). Such a result has a simple conceptual explanation. A perfect nonreciprocal isolator (lossy device) or phase shifter (lossless device) must be fully transparent from one side, meaning that it does not modify either the amplitude or the phase of the incident waves. Such functionality may seem impossible because it implies the absence of any wave scattering from the metasurface, while the currents in the meta-atoms are nonzero. However, in an artificial "moving" metasurface, the currents induced due to bianisotropic effects and due to the electric and magnetic polarizations of the meta-atoms cancel the scattering from each other and form a nonscattering system. Conceptually, such a metasurface resembles a thin layer with homogeneous and isotropic electric and magnetic properties moving outwards from the source of incident waves at the speed of light. This way, we emulate the situation where the incident waves simply cannot reach the layer, yielding zero scattering. When illuminated from the opposite direction, the layer will strongly scatter waves.

The modular decomposition shown in Fig. 6(a) allows us to immediately understand if the nonreciprocal meta-atom under analysis in fact has the necessary properties. At first glance, it seems that the meta-atom possesses polarization properties of all possible kinds and, therefore, is not suitable for implementation in metasurface-based isolators. However, if one assumes illumination of the meta-atom along the $+y$ direction with the polarization of the incident fields given by $\mathbf{E}_{inc} = -\mathbf{x}E_{inc}$ and $\mathbf{H}_{inc} = \mathbf{z}H_{inc}$ (the same assumption was made in Ref. [18]), the conclusion becomes the opposite. From the modular decomposition, one can make the following observations. Firstly, the artificial "moving" module is excited at its most, since the illumination is along its axis. Secondly, the twisted omega module is not excited, since the illumination is perpendicular to its axis. Thirdly, taking into account the orientation of $\mathbf{E}_{inc}$ ($\theta = 90^\circ$ and $\phi = 180^\circ$), the chiral and Tellegen bianisotropic effects are minimized. The latter observation can be also confirmed by examining the plots in Figs. 6(b) and 6(c), depicting the axial chiral and Tellegen polarizability components for different orientations of the incident electric field. The maximum of the chiral response is observed for $\theta = 90^\circ$ and $\phi = (45^\circ + 90^\circ N)$ (where N is an integer), while the maximum of the Tellegen properties is achieved for $\theta = 45^\circ$ and $\phi = 180^\circ N$.

Next, we apply the decomposition to the virtually moving meta-atom over a frequency sweep from 1.97 to 1.98 GHz. The results can be seen in the video file in the Supplemental Material [22]. From the video, it can be observed that the *weights* of the magnetic, chiral, and Tellegen modules in the decomposition are nearly not altered over the entire range (the absolute strengths of these modules, naturally, are maximized at the resonance). The electric module is decreased at high frequencies. All other modules change their weights in a way corresponding to the evolution of the real and imaginary parts during the transition through the Lorentzian peak.

Thus, modular decomposition of meta-atoms is a useful method to determine their polarization properties for all illumination directions. Three other examples of meta-atom decomposition, including a double-turn helix, a double split-ring resonator, and a nonreciprocal swastika-shaped inclusion, can be found in the Supplemental Material [22].

VI. DISCUSSION

The above examples clearly demonstrate the usefulness and potential of the modular-decomposition concept. Using relatively simple vector-algebra manipulations, one can analyze the polarization properties of an arbitrary meta-atom for all possible configurations of incident plane waves, identify *all* possible (under the assumption of a

linear dipolar response) scattering effects in this meta-atom, and find optimal excitations for maximizing or minimizing particular effects. Although the modular analysis reported in this paper is introduced based on the polarizability description, it is possible to extend it analogously to susceptibility characterization, which is beneficial for metasurfaces incorporating metal-backed dielectric layers.

The proposed analysis can be exploited not only for the analysis of existing meta-atoms and artificial composites based on them, but also as a starting point for meta-atom synthesis. Indeed, by tuning the geometrical parameters of a meta-atom and analyzing the resulting modifications of the conceptual modules in its decomposition, one can gain an insight into how to engineer the necessary polarization effects. Moreover, in numerical optimization of the shape and dimensions of meta-atoms, the decomposition developed provides qualitative and quantitative information showing the relative strengths of all scattering phenomena in this meta-atom, for arbitrary illuminations. Using these data, one can run an optimization algorithm, maximizing and/or minimizing the decomposition parameters which are relevant to specific synthesis goals.

In this paper, we perform modular decompositions only for the dipolar response, but this does not mean that within this framework all higher-order multipoles must be neglected. We expect that similar thinking can be applied in the future to understanding and optimizing multipole scattering and absorption.

ACKNOWLEDGMENTS

This work was supported by the Finnish Foundation for Technology Promotion and the Academy of Finland (Project 287894).

[1] D. R. Smith, J. B. Pendry, and M. C. K. Wiltshire, Metamaterials and negative refractive index, Science **305**, 788 (2004).
[2] A. Q. Liu, W. M. Zhu, D. P. Tsai, and N. I. Zheludev, Micromachined tunable metamaterials: A review, J. Opt. **14**, 114009 (2012).
[3] Tie Jun Cui, Microwave metamaterials, Natl. Sci. Rev. **5**, 134 (2018).
[4] Yuri Kivshar, All-dielectric meta-optics and non-linear nanophotonics, Natl. Sci. Rev. **5**, 144 (2018).
[5] Sophia R. Sklan and Baowen Li, Thermal metamaterials: Functions and prospects, Natl. Sci. Rev. **5**, 138 (2018).
[6] Stefan Mühlig, Christoph Menzel, Carsten Rockstuhl, and Falk Lederer, Multipole analysis of meta-atoms, Metamaterials **5**, 64 (2011).
[7] Martin Fruhnert, Ivan Fernandez-Corbaton, Vassilios Yannopapas, and Carsten Rockstuhl, Computing the T-matrix of a scattering object with multiple plane wave illuminations, Beilstein J. Nanotechnol. **8**, 614 (2017).
[8] Rasoul Alaee, Carsten Rockstuhl, and Ivan Fernandez-Corbaton, An electromagnetic multipole expansion beyond the long-wavelength approximation, Opt. Commun. **407**, 17 (2018).
[9] Rasoul Alaee, Carsten Rockstuhl, and Ivan Fernandez-Corbaton, Exact multipolar decompositions with applications in nanophotonics, Adv. Opt. Mater. **7**, 1800783 (2019).
[10] Charles William Bunn, *Chemical Crystallography: An Introduction to Optical and X-ray Methods* (Clerendon Press, Oxford, United Kingdom, 1961).
[11] Richard Williams, Optical rotatory power and linear electro-optic effect in nematic liquid crystals of p-azoxyanisole, J. Chem. Phys. **50**, 1324 (1969).
[12] A. A. Sochava, C. R. Simovski, and S. A. Tretyakov, in *Advances in Complex Electromagnetic Materials*, edited by A. Priou, A. Sihvola, S. Tretyakov, and A. Vinogradov, NATO ASI Series No. 28 (Springer Netherlands, Dordrecht, 1997), p. 85.
[13] A. Papakostas, A. Potts, D. M. Bagnall, S. L. Prosvirnin, H. J. Coles, and N. I. Zheludev, Optical Manifestations of Planar Chirality, Phys. Rev. Lett. **90**, 107404 (2003).
[14] E. Plum, X.-X. Liu, V. A. Fedotov, Y. Chen, D. P. Tsai, and N. I. Zheludev, Metamaterials: Optical Activity Without Chirality, Phys. Rev. Lett. **102**, 113902 (2009).
[15] Li Quan, Younes Ra'di, Dimitrios L. Sounas, and Andrea Alù, Maximum Willis Coupling in Acoustic Scatterers, Phys. Rev. Lett. **120**, 254301 (2018).
[16] Tobias Frenzel, Muamer Kadic, and Martin Wegener, Three-dimensional mechanical metamaterials with a twist, Science **358**, 1072 (2017).
[17] Ricardo Marqués, Francisco Medina, and Rachid Rafii-El-Idrissi, Role of bianisotropy in negative permeability and left-handed metamaterials, Phys. Rev. B **65**, 144440 (2002).
[18] A. Degiron and D. R. Smith, One-way glass for microwaves using nonreciprocal metamaterials, Phys. Rev. E **89**, 053203 (2014).
[19] Nanfang Yu and Federico Capasso, Flat optics with designer metasurfaces, Nat. Mater. **13**, 139 (2014).
[20] Stanislav B. Glybovski, Sergei A. Tretyakov, Pavel A. Belov, Yuri S. Kivshar, and Constantin R. Simovski, Metasurfaces: From microwaves to visible, Phys. Rep.: Rev. Sect. Phys. Lett. **634**, 1 (2016).
[21] Nader Engheta, Circuits with light at nanoscales: Optical nanocircuits inspired by metamaterials, Science **317**, 1698 (2007).
[22] See Supplemental Material at http://link.aps.org/supplemental/10.1103/PhysRevApplied.12.024059 for additional information.
[23] Permanent link for supporting files: https://github.com/picassonok/Materiatronics.
[24] Felipe Bernal Arango and A. Femius Koenderink, Polarizability tensor retrieval for magnetic and plasmonic antenna design, New J. Phys. **15**, 073023 (2013).
[25] Viktar S. Asadchy, Igar A. Faniayeu, Younes Ra'di, and Sergei A. Tretyakov, Determining polarizability tensors for an arbitrary small electromagnetic scatterer, Photonics Nanostruct. Fundam. Appl. **12**, 298 (2014).

[26] Mohammad Yazdi and Nader Komjani, Polarizability calculation of arbitrary individual scatterers, scatterers in arrays, and substrated scatterers, J. Opt. Soc. Am. B **33**, 491 (2016).
[27] X. X. Liu, Y. Zhao, and A. Alù, Polarizability tensor retrieval for subwavelength particles of arbitrary shape, IEEE Trans. Antennas Propag. **64**, 2301 (2016).
[28] Theodosios D. Karamanos and Nikolaos V. Kantartzis, Full polarizability matrix extraction formulas for electrically small particles via reflection/transmission coefficients, Progr. Electromagn. Res. **82**, 93 (2018).
[29] S. Tretyakov, A. Sihvola, and B. Jancewicz, Onsager-Casimir principle and the constitutive relations of bi-anisotropic media, J. Electromagn. Waves Appl. **16**, 573 (2002).
[30] Chen-To Tai, in *General Vector and Dyadic Analysis: Applied Mathematics in Field Theory* (IEEE, Piscataway, NJ, 1997).
[31] B. Sauviac, C. R. Simovski, and S. A. Tretyakov, Double split-ring resonators: Analytical modeling and numerical simulations, Electromagnetics **24**, 317 (2004).
[32] J. D. Baena, J. Bonache, F. Martin, R. M. Sillero, F. Falcone, T. Lopetegi, M. A. G. Laso, J. Garcia-Garcia, I. Gil, M. F. Portillo, and M. Sorolla, Equivalent-circuit models for split-ring resonators and complementary split-ring resonators coupled to planar transmission lines, IEEE Trans. Microw. Theory Tech. **53**, 1451 (2005).
[33] Viktar S. Asadchy, Ana Díaz-Rubio, and Sergei A. Tretyakov, Bianisotropic metasurfaces: Physics and applications, Nanophotonics **7**, 1069 (2018).
[34] Bernard D. H. Tellegen, The gyrator, a new electric network element, Philips Res. Rep. **3**, 81 (1948).
[35] E. O. Kamenetskii, On the technology of making chiral and bianisotropic waveguides for microwave propagation, Microw. Opt. Technol. Lett. **11**, 103 (1996).
[36] S. A. Tretyakov, S. I. Maslovski, I. S. Nefedov, A. J. Viitanen, P. A. Belov, and A. Sanmartin, Artificial Tellegen particle, Electromagnetics **23**, 665 (2003).
[37] Mamdouh M. I. Saadoun and Nader Engheta, A reciprocal phase shifter using novel pseudochiral or Ω medium, Microw. Opt. Technol. Lett. **5**, 184 (1992).
[38] Sergei A. Tretyakov, Nonreciprocal composite with the material relations of the transparent absorbing boundary, Microw. Opt. Technol. Lett. **19**, 365 (1998).
[39] ANSYS Electronics Desktop 2017.2: https://www.ansys.com/.
[40] MATLAB and Statistics Toolbox Release 2018a, The MathWorks, Inc., Natick, Massachusetts, USA.
[41] The linear scale of the antisymmetric modules (such as the twisted omega module) represents the strength of the polarization response to unpolarized incident waves propagating along the module's axis.
[42] Ranjan Singh, Eric Plum, Weili Zhang, and Nikolay I. Zheludev, Highly tunable optical activity in planar achiral terahertz metamaterials, Opt. Express **18**, 13425 (2010).
[43] A. Serdyukov, I. Semchenko, S. Tretyakov, and A. Sihvola, *Electromagnetics of Bi-Anisotropic Materials – Theory and Application* (Gordon and Breach Science Publishers, Amsterdam, 2001), Vol. 11, p. 131.
[44] Chihhui Wu, Nihal Arju, Glen Kelp, Jonathan A. Fan, Jason Dominguez, Edward Gonzales, Emanuel Tutuc, Igal Brener, and Gennady Shvets, Spectrally selective chiral silicon metasurfaces based on infrared Fano resonances, Nat. Commun. **5**, 3892 (2014).
[45] Y. Ra'di, V. S. Asadchy, and S. A. Tretyakov, One-way transparent sheets, Phys. Rev. B **89**, 075109 (2014).
[46] S. Taravati, B. A. Khan, S. Gupta, K. Achouri, and C. Caloz, Nonreciprocal nongyrotropic magnetless metasurface, IEEE Trans. Antennas Propag. **65**, 3589 (2017).